Amnon Yariv (S'56–M'59–F'70), for a photograph and biography, see p. 337 of the March 1982 issue of the JOURNAL OF QUANTUM ELECTRONICS.

Kam Y. Lau (M'78), for a photograph and biography, see p. 1361 of the September 1982 issue of the JOURNAL OF QUANTUM ELECTRONICS.

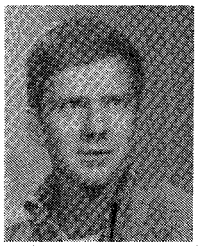

Nadav Bar-Chaim was born in Nathanya, Israel, in 1946. He received the B.Sc. degree in mathematics and physics from the Hebrew University, Jerusalem, Israel, in 1967, and the M.S. degree in physics and the Ph.D. degree in electrical engineering from Tel-Aviv University, Tel-Aviv, Israel, in 1973 and 1978, respectively.

In 1978 he joined the California Institute of Technology, Pasadena, as a Postdoctoral Fellow, where his work included research in semiconductor lasers and integrated optoelectronic circuits. In 1981 he joined Ortel Corporation, Alhambra, CA.

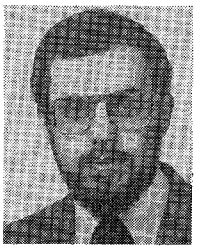

Israel Ury was born in St. Louis, MO, in 1956. He received the B.Sc. and M.S. degrees in electrical engineering from the University of California, Los Angeles, and the Ph.D. degree in applied physics from the California Institute of Technology, Pasadena, in 1975, 1976, and 1980, respectively.

While at the California Institute of Technology he was involved with research in integrated optoelectronics. Currently, he is President of Ortel Corporation, Alhambra, CA.

Optical Phase Modulation in an Injection Locked AlGaAs Semiconductor Laser

SOICHI KOBAYASHI, MEMBER, IEEE, AND TATSUYA KIMURA, SENIOR MEMBER, IEEE

Abstract—**Optical phase modulation obtained by injecting coherent CW light into a directly frequency-modulated semiconductor laser is reported. Phase modulation at up to a 1 GHz modulation frequency has been obtained without compression for a 1.4 GHz half locking bandwidth. Phase deviation can be represented by the ratio of the original FM deviation to the locking half bandwidth. The phase deviation normalized by the frequency deviation is inversely proportional to the cutoff modulation frequency. A static phase shift of π took place with a 0.48 mA drive current change in the injection locked laser.**

Reduction in FM noise by means of CW light injection and FM noise accumulation in cascaded injection locked laser amplifiers are discussed, together with the optimum design for an injection locked repeater system.

I. INTRODUCTION

COHERENT optical transmission systems are attractive as future systems with wide repeater spacing and large information capacity [1]. The amplitude, frequency, or phase of the coherent optical carrier is modulated and then demodulated through a homodyne or heterodyne scheme. The possibility of a coherent FSK signal transmission system using a semiconductor laser transmitter and an independent local oscillator for heterodyning has successfully been demonstrated [2]. A coherent PSK signal transmission system is desired as a more advanced technology because of the low receiving power level in the PSK-homodyne or -heterodyne detection scheme [1].

Manuscript received February 17, 1982.

The authors are with the Musashino Electrical Communication Laboratory, Nippon Telegraph and Telephone Public Corporation, Musashino-shi, Tokyo, Japan.

Injection locking in semiconductor lasers has been studied [3], [4] for coherent optical system applications. The bandwidth-versus-gain relation of injection locked semiconductor laser amplifiers, amplification of FM optical signals, and single mode operations in directly modulated semiconductor lasers injected with CW light, have been reported [5]–[10].

Direct optical frequency modulation in semiconductor lasers has been demonstrated and the broad-band modulation frequency characteristics of different types of laser structures have been studied [11], [12].

The present paper reports experimental studies on optical phase modulation (PM) obtained by injecting CW coherent light into a directly frequency-modulated (FM) AlGaAs double heterostructure semiconductor laser. Measurement systems and procedures for the induced PM will be described in Section II. In Section III, the results obtained in the static phase shift and dynamic PM modulation by injection locking will be shown. Analytical treatment will be described in Section IV. Reduction in semiconductor laser FM noise by injection locking will be discussed in Section V.

II. MEASUREMENT SYSTEMS AND PROCEDURES

A. Experimental Setup

An experimental setup to study phase modulation is shown in Fig. 1. Two double heterostructure AlGaAs semiconductor lasers (*LD*1, *LD*2), with an identical cavity length, operate continuously in a single longitudinal mode at 840 nm. These lasers have channeled substrate planar (CSP) geometry [13]. Their oscillation thresholds are $I_{th,1} = 62$ mA and $I_{th,2} = 6$ mA. They are mounted individually on copper heat sinks whose

0018-9480/82/1000-1650$00.75

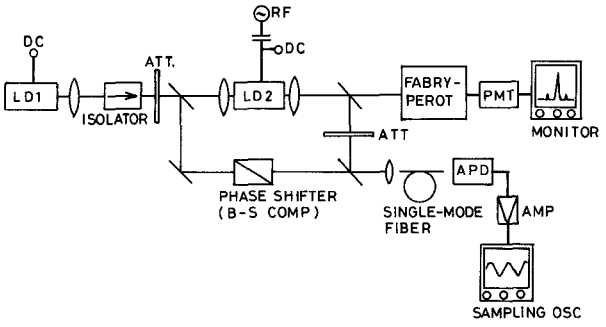

Fig. 1. Configuration for optical phase modulation experiment using optical injection locking. Mach-Zehnder interferometer and scanning Fabry-Perot interferometer are used to measure the phase modulation.

temperatures are stabilized within a ±0.05°C accuracy by means of thermoelectric elements. The *LD*1 output is collimated with antireflection-coated microlenses and injected into *LD*2. Back reflected light from *LD*2 to *LD*1 is eliminated by two optical isolators arranged in tandem, with 40 dB isolation [14]. Longitudinal mode frequency tuning of two lasers and their coupling efficiency measurement are carried out by the method reported earlier [3], [15]. The locking bandwidth can be measured by changing the *LD*1 current as has been reported [3].

The scanning Fabry-Perot (FP) interferometer, shown in Fig. 1, is used to measure the modulation sideband spectra. The Mach-Zehnder (MZ) interferometer configuration is used for PM measurement. The attenuator balances the light amplitudes in two branches of the interferometer, and the Babinet-Soleil (BS) compensator acts as a phase shifter to calibrate the phase deviation. The path difference between the two branches of the interferometer is made less than 1.4 mm. The single mode fiber ensures wavefront matching of CW and PM light at the surface of the Si-APD.

B. Static Phase Shift

First, the two lasers are oscillated continuously without applying an RF signal. Change of the *LD*2 resonant frequency by changes of its drive current causes a static phase shift with respect to the injected light wave. The static phase shift versus *LD*2 resonant frequency shift relation is measured by homodyne detection using the MZ interferometer configuration.

C. Induced PM Signal Measurement

An RF sinusoidal signal with frequency f_m is superimposed on the *LD*2 bias current for direct current modulation.

Without injection, *LD*2 emits optical FM signals as

$$E_{\mathrm{FM}} = E_0 \exp\{j[2\pi f_0 t + \beta \sin(2\pi f_m t)]\},$$
$$\beta = \Delta F / f_m. \tag{1}$$

Here, ΔF is the maximum frequency deviation (MFD), f_0 is the optical carrier frequency, and β is the frequency modulation index.

When CW light is injected into *LD*2, MFD is suppressed [16]. Simultaneously, the phase modulation (PM) signal is induced with the injection. The PM signal is represented as

$$E_{\mathrm{PM}} = E_0 \exp\{j[2\pi f_0 t + \Delta\Phi \sin(2\pi f_m t)]\}. \tag{2}$$

Here, $\Delta\Phi$ is the maximum phase deviation (MPD). In ideal PM, $\Delta\Phi$ does not change when f_m is changed.

The induced PM signal is observed on the display of the sampling oscilloscope through the MZ interferometer. The optical phase bias is adjusted by the BS compensator to obtain a sinusoidal signal on the display. The MPD is calibrated by the known phase shift of the BS compensator. It can also be measured by the FP interferometer using the same method as was reported earlier [11], [12]. Results obtained by both methods are compared with the measured FM index without injection in the following sections.

In dynamic phase shift measurement, frequency characteristics of the Si-APD have been calibrated by using a beat note between the two lasers, both under CW drive conditions. The 3 dB down cutoff frequency measured was about 500 MHz. Frequency characteristics of the *LD*2 drive curcuit were obtained from the above Si-APD characteristics assuming that the *LD*2 has flat frequency characteristics for small current modulation. The cutoff frequency measured was 600 MHz. The frequency characteristics of the drive and detection circuits have been compensated for in order to obtain the intrinsic PM performance over a wide modulation frequency range.

III. Experimental Results

A. Static Phase Shift

Two lasers, *LD*1 and *LD*2, are driven by dc currents $I_1 = 1.5 \times I_{\mathrm{th},1}$ and $I_2 = 1.54 \times I_{\mathrm{th},2}$, respectively. Injected CW light power in *LD*2 is $P_{\mathrm{in}} = -22$ dBm. A static phase shift of π takes place when the *LD*2 bias current is changed by 0.48 mA, as shown in Fig. 2. The full locking bandwidth $2\Delta f$ is 1.4 GHz. The phase shift curve obtained between $-\pi/2$ and $\pi/2$ is nearly linear, rather than sinusoidal.

Visibility of the MZ interferometer output is more than 95 percent when the BS compensator and the attenuator are adjusted at the *LD*2 cavity center in a locking state. Measured visibility was between 74 and 89 percent in relation to that of the MZ interferometer. The visibility becomes large when the locking bandwidth, which is determined by the *LD*2 bias current, injected power, and cavity Q becomes broad. Power injected into *LD*2 was varied between -33 and -22 dBm. The phase between the injected and output waves shifts proportionally to the *LD*2 drive current. The measured phase shift normalized by the *LD*2 cavity frequency shift is shown in Fig. 3 as a function of the locking half bandwidth. The experimental result is in good agreement with the theoretical line, which will be derived in Section IV. This result shows that, in order to increase the phase shift per unit drive current in static operation, the locking bandwidth should be narrow.

B. Phase Modulation

When *LD*2 is driven by an RF current and CW light is injected, a phase modulation output is obtained. Fig. 4 shows the frequency spectra of 1) PM modulation with, 2) FM modulation without injection measured by the FP interferometer, and 3) a PM signal converted by the MZ interferometer [16]. Modulation frequency f_m is 300 MHz. Direct drive currents are

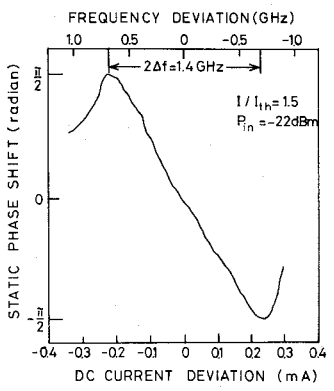

Fig. 2. Static phase shift obtained by changing the $LD2$ oscillator frequency with respect to that of $LD1$ through the bias current.

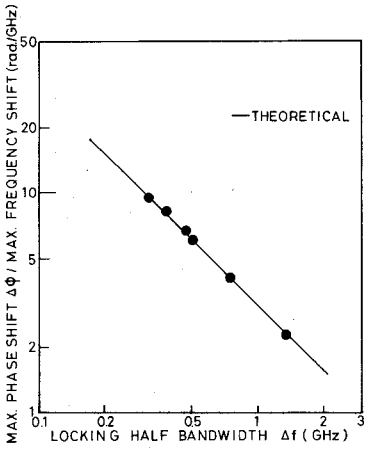

Fig. 3. Maximum phase shift per unit frequency deviation as a function of the locking half bandwidth. Solid line shows the relation $\Delta\Phi/(f_0 - f_{in}) = 1/\Delta f$.

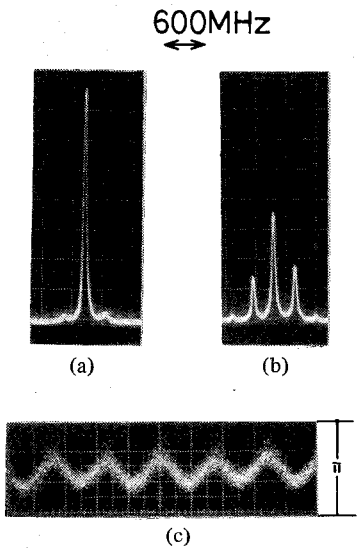

Fig. 4. Frequency spectra and phase deviation. (a) PM spectrum with −28 dBm power injection. Maximum phase deviation $\Delta\Phi = 0.17$ rad/mA. (b) FM spectrum without injection. FM index $\Delta F/f_m = 0.47$/mA. (c) PM signal measured by MZ interferometer $\Delta\Phi = 0.17$ rad/mA.

$I_1 = 1.6 \times I_{th,1}$ and $I_2 = 1.34 \times I_{th,2}$. The modulation current is 2 mA_{0-p}. Measured frequency deviation is 130 MHz/mA in Fig. 4(b). Modulation index, which is defined by $\beta = \Delta F/f_m$, is suppressed from 0.47 to 0.17 per mA by injecting −28 dBm CW power. The maximum phase deviation (MPD) per unit drive current is 0.17 rad/mA for the locking half bandwidth of $\Delta f = 800$ MHz. The MPD measured by sideband amplitudes in Fig. 4(a) coincides with that indicated in Fig. 4(c).

Fig. 5 shows the modulation frequency characteristics between 100 MHz and 1.3 GHz of PM signals. $LD2$ bias currents are 1) $1.15 \times I_{th,2}$, 2) $1.35 \times I_{th,2}$, and 3) $1.55 \times I_{th,2}$. Here the lowest modulation frequency is chosen at around 100 MHz, at which only the purely electronic contribution is effective in angular modulation, as will be seen in Fig. 7. Injected powers are varied between −40 and −22 dBm. The ordinate at the left-hand side shows MPD per unit drive current with injection and that at the right-hand side indicates FM index per unit current without injection. Closed circles and broken line curves show values of experimental and theoretical FM indexes per unit current [11], [12]. Other symbols and lines show results of MPD per unit current for each locking bandwidth. Theoretical MPD curves will be explained in Section IV. Small vertical bars on the curves show the locking half bandwidth for each experimental condition. The FM index decreases with increases of the modulation frequency as seen in (1). The slope becomes gradual at frequencies higher than 500 MHz because of the carrier resonant phenomenon [12]. The MPD curves tend to approach the FM index curve at high modulation frequencies and the MPD becomes constant at low modulation frequencies. As the locking bandwidth becomes broad, the MPD per unit RF current becomes small, and the cutoff frequency f_{mc}, at which the MPD decreases to $1/\sqrt{2}$, becomes high. The MPD becomes small at large $LD2$ bias current.

The result of Fig. 5(b) is rearranged in Fig. 6 to show the MPD dependence in the injected power level or the locking bandwidth. The parameter is the modulation frequency f_m. At high injected power levels, MPD tends to be asymptotic to the low modulation frequency line. The high frequency MPD saturates at relatively high injection levels, while the low frequency MPD increases as the injection level decreases.

Fig. 7 shows the frequency characteristics of MPD per unit current at $1.5 \times I_{th,2}$ bias current from 1 kHz to 1.3 GHz. Open circles show the experimental results. The solid curve shows the theoretical PM deviation. The broken line and the dot-and-broken line show theoretical thermal and carrier effect curves calculated from the FM deviation in Section IV. Experimental results are well fitted to those theoretical curves over the wide modulation frequency range.

IV. Theory

A. Analytical Formulation

The van der Pol equation, assuming that the spontaneous emission term can be neglected, is given as follows [3], [17]:

$$d\Phi/dt = (E_{in}/E_\varrho)\sin(\Psi - \Phi)/2\tau_p - \Delta\omega + d\Theta/dt \tag{3}$$

$$S_\varrho = E_\varrho^2,$$

$$P_{in} = E_{in}^2,$$

$$\Delta\omega = \omega_{in} - \Omega_0 (= \omega_\varrho - \Omega_0). \tag{4}$$

Here, S_ϱ is the photon density, τ_p is photon lifetime, P_{in} is the injected photon density, E_ϱ is the locked electric field amplitude, E_{in} is the injected electric field amplitude, ω_{in} is injection light angular frequency, ω_ϱ is the locked angular frequency, and Ω_0 is the cavity angular frequency of the resonator of LD_2. In an injection locked state, $\omega_{in} = \omega_\varrho$. Φ is the phase of

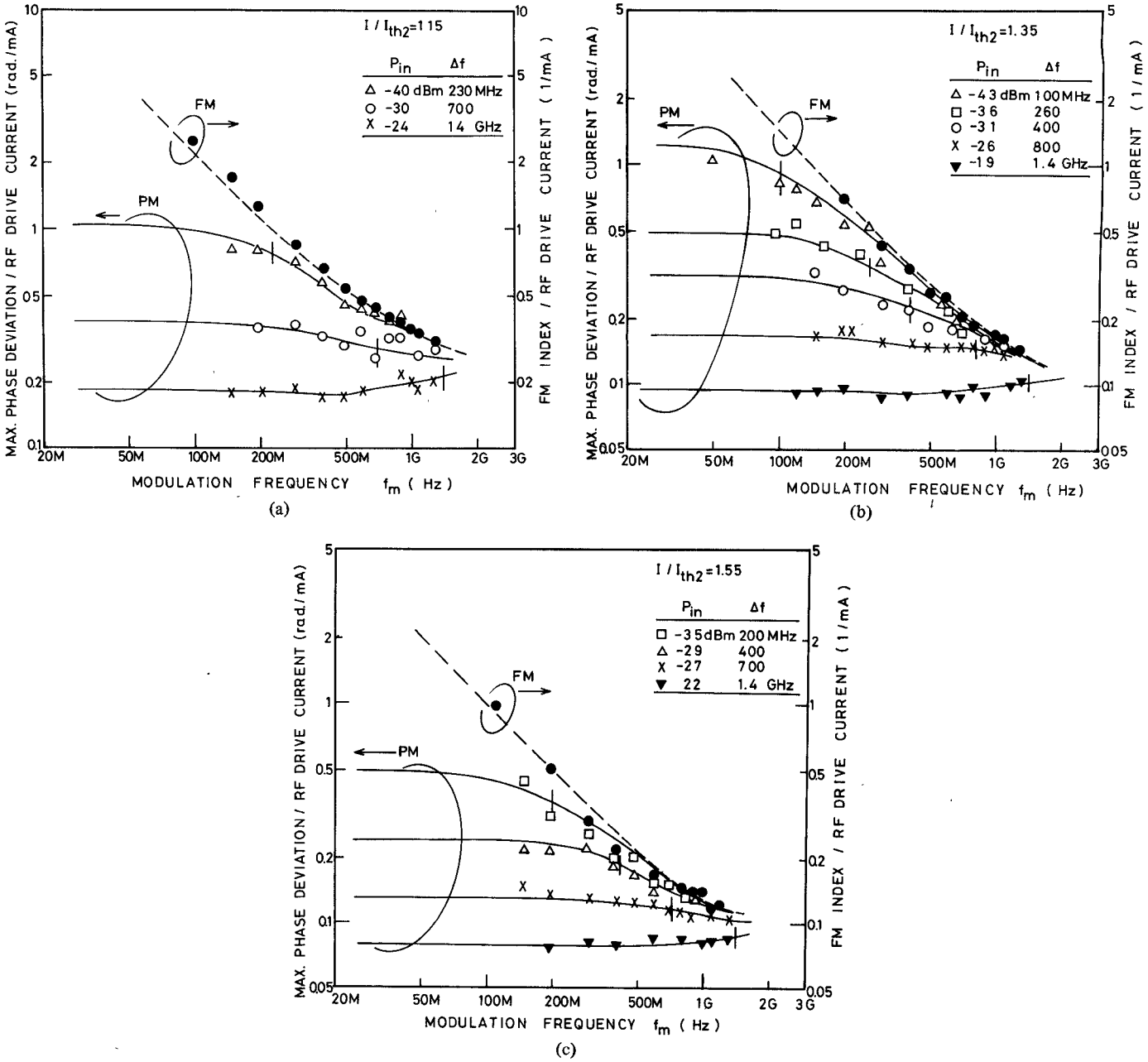

Fig. 5. Maximum phase deviation characteristics. (a) Bias current is $1.15 \times I_{th,2}$, (b) $1.35 \times I_{th,2}$, and (c) $1.55 \times I_{th,2}$. Closed circles and broken lines show experimental and calculated results of maximum frequency deviation without injection. Solid lines show theoretical values for PM.

the locked signal, Θ is the phase of the free running laser (LD_2), and Ψ is the phase of the injection signal from LD_1.

First-order perturbation equation is obtained assuming the following:

$$\begin{aligned} S_\ell &= S_0 + S_1 \cong E_0^2 + 2E_1E_0, \\ E_\ell &= E_0 + E_1, \\ E_{in} &= E_{i0} + E_{i1}, \\ \Phi &= \Phi_0 + \Delta\Phi, \\ \Theta &= \Theta_0 + \Delta\Theta, \\ \Psi &= \Psi_0 + \Delta\Psi. \end{aligned} \tag{5}$$

Here, suffixes 0 and 1 mean dc and first-order perturbation. Substituting (5) into (3), the first-order perturbation rate equation is obtained as follows:

$$\begin{aligned} j\omega\Delta\Phi = \{&[E_{i1}\sin(\Psi_0 - \Phi_0) + E_{i0}(\Delta\Psi - \Delta\Phi) \\ &\cdot \cos(\Psi_0 - \Phi_0)]/2\tau_p - \Delta\omega E_1 - j\omega\Delta\Theta E_0\}/E_0. \end{aligned} \tag{6}$$

At the center frequency of the $LD2$ cavity, $\Delta\omega = 0$ and $\Psi_0 = \Phi_0$. By substituting these conditions into (6), one obtains

$$\begin{aligned} j\omega\Delta\Phi &= [E_{i0}(\Delta\Psi - \Delta\Phi)/2\tau_p - j\omega\Delta\Theta E_0]/E_0 \\ \Delta\Phi &= (E_{i0}\Delta\Psi/2\tau_p - j\omega\Delta\Theta E_0)/(E_{i0}/2\tau_p + j\omega E_0) \\ &= (\Delta\Psi\Delta f - jf_m\Delta\Theta)/(\Delta f + jf_m). \end{aligned} \tag{7}$$

Here, $\Delta f = (E_{i0}/E_0)/4\pi\tau_p = \sqrt{P_{in}/S_\ell}/4\pi\tau_p$ is the locking half bandwidth (LHB). Phase excursion $\Delta\Phi$ is represented as

$$\Delta\Phi = \sqrt{[\Delta\Psi^2 + (f_m/\Delta f)^2\,\Delta\Theta^2]/[1 + (f_m/\Delta f)^2]}. \tag{8}$$

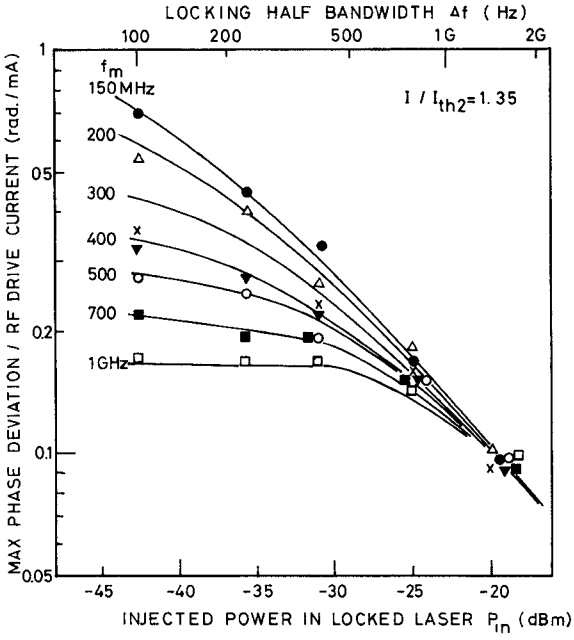

Fig. 6. Maximum phase deviation as a function of input power or locking half bandwidth.

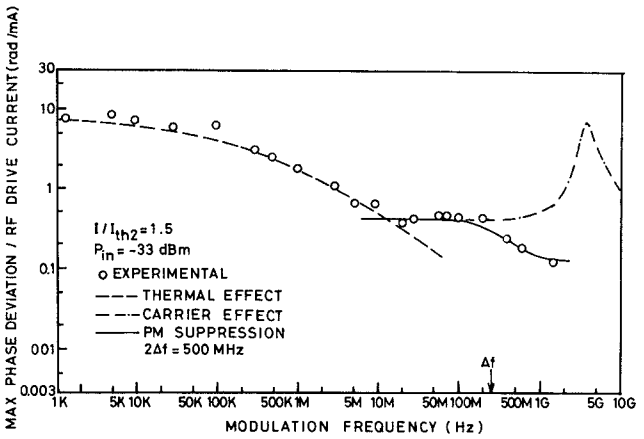

Fig. 7. Frequency characteristics of the maximum phase deviation.

For small signal phase deviation $\Delta\Psi$ compared with the modulated laser phase deviation $\Delta\Theta$, (8) is approximated by

$$\Delta\Phi = \Delta\Theta\sqrt{(f_m/\Delta f)^2/[1+(f_m/\Delta f)^2]}. \tag{9}$$

When CW light is injected into the directly FM modulated laser, the modulation index is suppressed by the factors [18], [19]

$$\beta_{out}/\beta_a = \Delta\Phi/\Delta\Theta = \sqrt{(f_m/\Delta f)^2/[1+(f_m/\Delta f)^2]}. \tag{10}$$

Here, β_{out} is the modulation index of locked output with CW light injection and β_a is the modulation index without injection.

The phase deviation can be represented by (9) with $\Delta\Theta = \beta_a = \Delta F/f_m$ [16]

$$\Delta\Phi = \Delta F\sqrt{1/(\Delta f^2 + f_m^2)}. \tag{11}$$

Fig. 8 shows the modulation index suppression ratio (10) and the maximum phase deviation (11) as a function of $f_m/\Delta f$.

B. Static Phase Shift

The static phase relation is represented from (3) as

$$(E_{i0}/E_0)\sin(\Psi_0 - \Phi_0)/2\tau_p - \Delta\omega = 0. \tag{12}$$

When the injected light has a frequency f_{in} which is identical

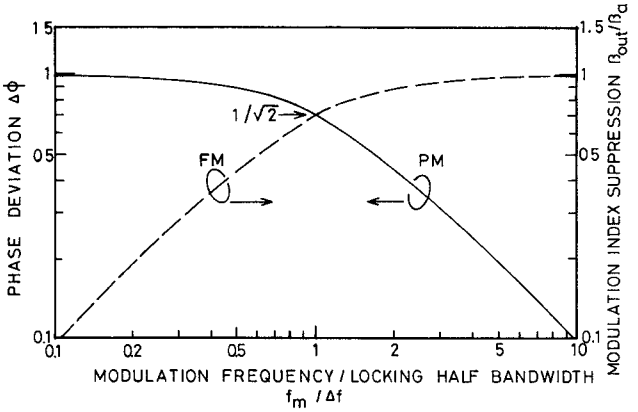

Fig. 8. Maximum phase deviation and FM index suppression characteristics as a function of modulation frequency normalized by the locking half bandwidth.

to the *LD*2 cavity center frequency f_c and a constant phase Ψ_0, which is arbitrarily chosen to be 0, the phase of the locked laser becomes

$$\Phi_0 = \sin^{-1}[(E_0/E_{i0})4\pi\tau_p(f_0 - f_{in})]. \tag{13}$$

As f_0 is shifted by means of the drive current, Φ_0 is changed because f_{in} is fixed to the cavity center. Φ_0 is changed by $\pm\pi/2$ from 0, when the frequency shift $f_{in} - f_0$ is equal to the locking half bandwidth

$$f_{in} - f_0 = (E_{i0}/E_0)/4\pi\tau_p = \Delta f. \tag{14}$$

At around $f_{in} = f_0$, the phase can be approximated by a linear function

$$\Phi_0 = (E_0/E_{i0})4\pi\tau_p(f_0 - f_{in}). \tag{15}$$

Experimental results in Fig. 2 show the linear phase shift characteristics near the cavity center frequency. The solid line in Fig. 3 represents

$$\Delta\Phi/(f_0 - f_{in}) = 1/\Delta f \tag{16}$$

which is derived from (15).

C. Phase Modulation

The maximum phase deviation $\Delta\Phi$ normalized by the maximum frequency deviation ΔF is shown in Fig. 9 as a function of modulation frequency f_m. The broken line shows the FM index $\beta = \Delta F/f_m = 1$. Solid lines, calculated from (11), show that $\Delta\Phi$ is constant at $\Delta F/\Delta f$ for f_m lower than the locking half bandwidth Δf, while it tends to be small at $f_m > \Delta f$. Experimental results, replotted from Fig. 5(b) indicate good agreement, again. Solid lines in Fig. 5(a)-(c) were also calculated from (11) by substituting the maximum frequency deviation without injection [12]. This figure, as well as Fig. 7, tells us that in order to get flat PM characteristics over a broad modulation frequency range, injection power, or equivalently, the locking half bandwidth, should be increased.

The solid line in Fig. 7 is calculated from (11) by substituting the measured maximum frequency deviation values and LHB. The broken line shows the relation $\Delta\Phi = \Delta F/\Delta f$ where ΔF is the theoretical value obtained from the thermal refractive index change by calculating the thermal conduction of each layer in the AlGaAs laser [12]. The dot-and-broken line shows the same relation $\Delta\Phi = \Delta F/\Delta f$ where ΔF is the theoretical value obtained from the carrier refractive index change considering lateral carrier diffusion in the CSP laser [12].

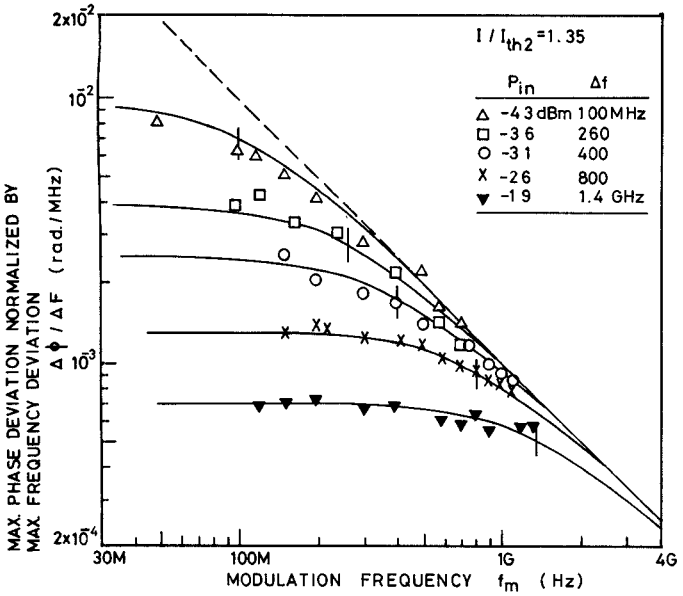

Fig. 9. Maximum phase deviation normalized by FM deviation as a function of the modulation frequency. Broken line shows the FM index $\beta = 1$.

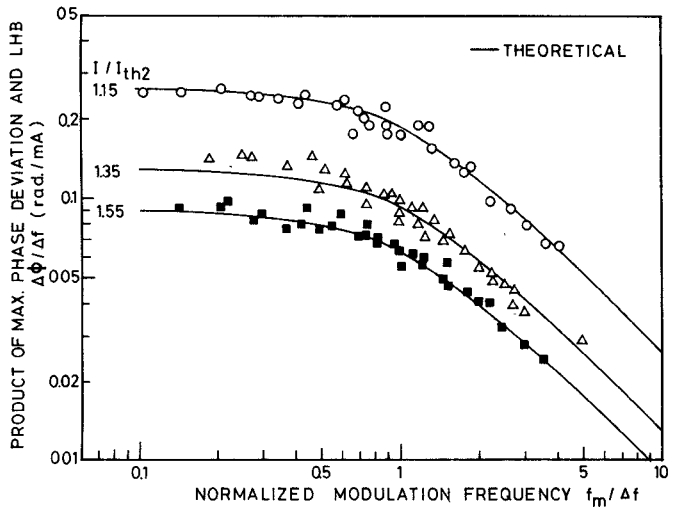

Fig. 10. Product of maximum phase deviation and locking half bandwidth as a function of normalized modulation frequency.

Fig. 10 shows the product of MPD and LHB as a function of the modulation frequency normalized by LHB. Direct drive currents are 1.15, 1.35, and 1.55 $\times I_{th,2}$. These results are reported from Fig. 5(a)-(c). The solid lines are the theoretical curves calculated by (11). This shows that MPD decreases as the dc drive current increases. This trend can be explained by the decreased frequency deviation in uninjected lasers at a high bias level [12].

Fig. 11 shows the MPD normalized by the MFD at the cutoff modulation frequency f_{mc} as a function of the cutoff frequency. Here, the cutoff frequency means the frequency at which MPD falls to $1/\sqrt{2}$ of the low modulation frequency value. The solid line shows the theoretical values calculated by (11) when $f_{mc} = \Delta f$. Experimental results for low cutoff frequency show good agreement with the straight line. In high f_{mc}, however, MFD is affected by the carrier resonant characteristics [12]. When f_{mc} is equal to Δf, ΔF shows constant frequency characteristics. The laser diode structure design to obtain a large ΔF has been discussed in a previous publication [12]. A high injection power level is desired to obtain high f_{mc} or Δf.

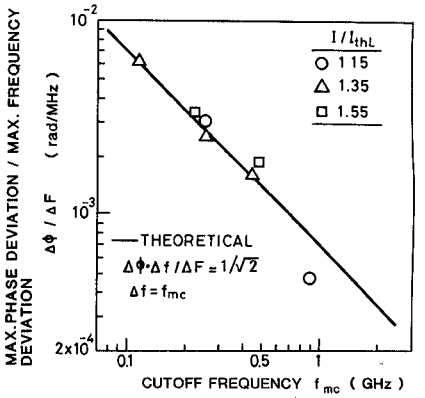

Fig. 11. Maximum phase modulation normalized by maximum frequency as a function of the cutoff frequency.

V. Discussion

A. Angular Noise Suppression

If we regard the modulation sideband as a component of angular modulation noise in the semiconductor laser, the phenomenon discussed so far can be regarded as the suppression of FM noise by optical injection. Fig. 12 shows frequency characteristics of modulation index suppression. The suppression is expressed by the ratio β_{out}/β_a, where β_{out} is the modulation index of the locked output with CW light injection and β_a is the modulation index without injection. The value of β_a between 1.4 and 0.14 corresponds to f_m between 100 MHz and 1.3 GHz. Experimental results in the figure are replotted again from Fig. 5(b). Solid lines show theoretical curves calculated from (10).

The angular modulation component is suppressed strongly as the LHB Δf increases. Fig. 13 shows the β_{out}/β_a as a function of modulation frequency normalized by LHB. All experimental results can be fitted to the unified theoretical curve given by (10).

B. Cascade Injection Locked Laser Amplifiers

Based on these results, it is necessary to discuss the FM noise suppression or accumulation characteristics in cascaded injection locked semiconductor laser amplifiers. Here again, we regard the modulation sideband as representing a noise component.

The FM suppression in FM signal amplification was obtained [10], [24] as follows:

$$\beta_{out}/\beta_{in} = \{1/[1 + (f_m/\Delta f)^2]\}^{1/2} = F_1 = (\overline{\Delta f_{out}^2}/\overline{\Delta f_{in}^2})^{1/2}. \quad (17)$$

Here, $\overline{\Delta f_{out}^2}$ and $\overline{\Delta f_{in}^2}$ are FM noise power of the locked laser output and input when FM signal is injected into the dc biased laser amplifier. The FM index suppression with CW light injection is represented by (10)

$$\beta_{out}/\beta_a = (\overline{\Delta f_{out}^2}/\overline{\Delta f_a^2})^{1/2} = F_2. \quad (10')$$

Here, $\overline{\Delta f_a^2}$ is the noise power of the laser output without injection. FM noise properties in cascaded locked amplifier repeaters of the coherent FSK system [10], [24] are obtained by comparing (17) and (10')

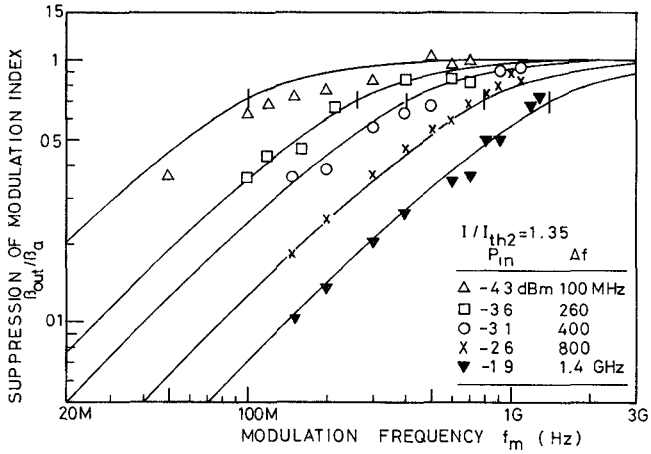

Fig. 12. Frequency characteristics of the modulation index suppression.

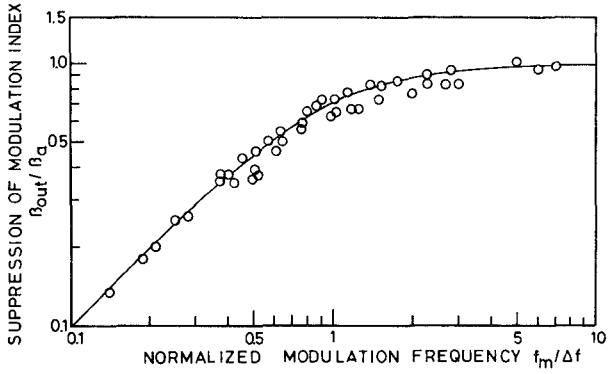

Fig. 13. Modulation index suppression as a function of modulation frequency normalized by the locking half bandwidth.

$$(\overline{\Delta f^2_{out}})_N = (\overline{\Delta f^2_a})_N \times F_2^2 + (\overline{\Delta f^2_{in}})_N \times F_1^2,$$
$$(\overline{\Delta f^2_{in}})_N = (\overline{\Delta f^2_{out}})_{N-1}. \quad (18)$$

Here, N denotes the number of cascade injection locked amplifiers.

Fig. 14 shows the FM noise power calculated using (18) when the injection locked amplifiers are connected in series, assuming that each locked amplifier has the same FM noise power. The top broken line shows the FM noise power of the locked amplifier and the bottom broken line shows that of the injected signal. The ratio of those FM noise powers is assumed to be 4×10^3 from experimental results. The FM noise of the semiconductor laser is caused by the thermal and mechanical cavity length change, and the refractive index change caused by mixed spontaneous light emissions into a lasing mode.

In Fig. 14, the frequency characteristics of FM noise power are assumed to be flat up to the 3 dB down cutoff frequency f_r. Calculated results show that FM noise power of the injection locked amplifier is reduced to the input FM noise power if the locking half bandwidth Δf is larger than the frequency bandwidth of the baseband signal bandwidth. Residual FM noise power, however, increases as the number of the locked amplifiers increases.

It is possible to reduce the FM noise power $\overline{\Delta f^2_{in}}$ further by the frequency stabilization technique [25], [26]. In such a case, the accumulated FM noise would be reduced still lower than the present result.

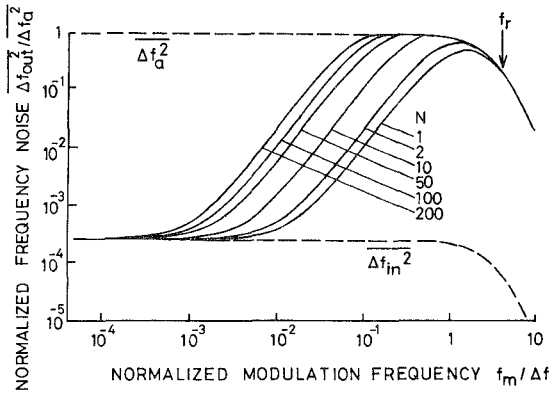

Fig. 14. Cumulative FM noise increase in cascade injection locked amplifiers. $\overline{\Delta f_a^2}$: FM noise of the locked amplifiers; f_r: 3 dB down frequency of Lorentzian distribution of $\overline{\Delta f_a^2}$; $\overline{\Delta f_{in}^2}$: FM noise of injected signal. N is the number of the locked amplifiers.

VI. Conclusion

Phase modulation is obtained in a CW light injected semiconductor laser. A static phase shift of π has been obtained by changing the injected light frequency over the full locking bandwidth. Frequency characteristics of the phase modulation are experimentally obtained and analytically explained by the van der Pol equation. The main features are characterized by FM deviation and locking bandwidth. FM noise reduction by coherent CW light injection is discussed and noise accumulation in cascaded injection locked amplifiers is calculated.

The phase modulation obtained in this paper has such advantages for future coherent optical transmission systems as: 1) narrow carrier linewidth due to frequency stabilized light injection and 2) high frequency modulation capability within a wide locking bandwidth.

References

[1] Y. Yamamoto and T. Kimura, "Coherent optical fiber transmission systems," *IEEE J. Quantum Electron.*, vol. QE-17, pp. 919–935, June 1981.

[2] S. Saito, Y. Yamamoto, and T. Kimura, "Optical FSK heterodyne detection experiments using semiconductor laser transmitter and local oscillator," *IEEE J. Quantum Electron.*, vol. QE-17, pp. 935–941, June 1981.

[3] S. Kobayashi and T. Kimura, "Injection locking in AlGaAs semiconductor laser," *IEEE J. Quantum Electron.*, vol. QE-17, pp. 681–689, May 1981.

[4] K. Otsuka and S. Tarucha, "Theoretical studies on injection locking and injection-induced modulation of laser diodes," *IEEE J. Quantum Electron.*, vol. QE-17, pp. 1515–1521, Aug. 1981.

[5] S. Kobayashi and T. Kimura, "Injection locking characteristics of an AlGaAs semiconductor laser," *IEEE J. Quantum Electron.*, vol. QE-16, pp. 915–917, Sept. 1980.

[6] —, "Coherence of injection phase-locked AlGaAs semiconductor laser," *Electron. Lett.*, vol. 16, pp. 915–917, Sept. 1980.

[7] S. Kobayashi, J. Yamada, S. Machida, and T. Kimura, "Single-mode operation of 500 Mbit/s modulated AlGaAs semiconductor laser by injection locking," *Electron. Lett.*, vol. 16, pp. 746–748, Sept. 1980.

[8] J. Yamada, S. Kobayashi, H. Nagai, and T. Kimura, "Modulated single-longitudinal mode semiconductor laser and fiber transmission characteristics," *IEEE J. Quantum Electron.*, vol. QE-17, pp. 1006–1009, June 1981.

[9] J. Yamada, S. Kobayashi, S. Machida, and T. Kimura, "Improve-

ment in intensity fluctuation noise of a 1 GHz-modulated InGaAsP laser by a light injection technique," *Japan. J. Appl. Phys.*, vol. 16, pp. L689-L692, Nov. 1980.
[10] S. Kobayashi, Y. Yamamoto, and T. Kimura, "Optical FM signal amplification and FM noise reduction in an injection locked AlGaAs semiconductor laser," *Electron. Lett.*, vol. 17, pp. 849-851, Oct. 1981.
[11] S. Kobayashi, Y. Yamamoto, and T. Kimura, "Modulation frequency characteristics of directly optical frequency modulated AlGaAs semiconductor laser," *Electron. Lett.*, vol. 17, pp. 350-351, May 1981.
[12] S. Kobayashi, Y. Yamamoto, M. Ito, and T. Kimura, "Direct frequency modulation in AlGaAs semiconductor lasers," *IEEE J. Quantum Electron.*, vol. QE-18, pp. 582-595, Apr. 1982.
[13] K. Aiki, M. Nakamura, T. Kuroda, and J. Umeda, "Channeled-substrate planar structure (AlGa)As injection lasers," *Appl. Phys. Lett.*, vol. 30, pp. 649-651, June 1977.
[14] K. Kobayashi and M. Seki, "Microoptic grating multiplexers and optical isolators for fiber-optic communications," *IEEE J. Quantum Electron.*, vol. QE-16, pp. 11-22, Jan. 1980.
[15] S. Kobayashi and T. Kimura, "Gain and saturation power of resonant AlGaAs laser amplifier," *Electron. Lett.*, vol. 16, pp. 230-232, Mar. 1980.
[16] ——, "Optical phase modulation in an injection locked AlGaAs semiconductor laser," *Electron. Lett.*, vol. 18, pp. 210-211, Mar. 1982.
[17] O. Hirota and Y. Suematsu, "Noise properties of injection lasers due to reflected waves," *IEEE J. Quantum Electron.*, vol. QE-15, pp. 142-148, Mar. 1979.
[18] M. Heines, J. C. Collinet, and J. G. Ondria, "FM noise suppression of an injection phase-locked oscillator," *IEEE Trans. Microwave Theory Tech.*, vol. MTT-16, pp. 738-742, Sept. 1968.
[19] T. Isobe and M. Tokida, "A new microwave amplifier for multichannel FM signal using a synchronized oscillator," *IEEE J. Solid-State Circuits*, vol. SC-4, pp. 400-408, Dec. 1969.
[20] F. R. Nash, "Mode guidance parallel to the junction plane of double-heterostructure GaAs lasers," *J. Appl. Phys.*, vol. 44, pp. 4696-4707, Oct. 1973.
[21] G. H. Thompson, "A theory for filamentation in semiconductor lasers including the dependence of dielectric constant on injected carrier density," *Opt. Electron.*, vol. 4, pp. 257-310, Aug. 1972.
[22] Y. Mitsuhashi, J. Shimada, and S. Mitsutsuka, "Voltage change across the self-coupled semiconductor laser," *IEEE J. Quantum Electron.*, vol. QE-17, pp. 1216-1225, July 1981.
[23] C. J. Buczek and R. J. Freiberg, "Hybrid injection locking of higher power CO_2 lasers," *IEEE J. Quantum Electron.*, vol. QE-8, pp. 641-650, July 1972.
[24] S. Kobayashi and T. Kimura, "Optical FM signal amplification by injection locked and resonant type semiconductor laser amplifier," *IEEE J. Quantum Electron.*, vol. QE-18, pp. 575-581, Apr. 1982.
[25] S. Saito and Y. Yamamoto, "Direct observation of Lorentzian lineshape of semiconductor laser and linewidth reduction with external grating feedback," *Electron. Lett.*, vol. 17, pp. 325-327, Apr. 1981.
[26] O. Nilsson, S. Saito, and Y. Yamamoto, "Oscillation frequency linewidth reduction and frequency modulation characteristics for a diode laser with external grating feedback," *Electron. Lett.*, vol. 17, pp. 589-591, Aug. 1981.

Soichi Kobayashi (M'80), for a photograph and biography, see p. 427 of the April 1982 issue of this TRANSACTIONS.

Tatsuya Kimura (S'63-M'68-SM'78), for a photograph and biography, see p. 65 of the January 1982 issue of the JOURNAL OF QUANTUM ELECTRONICS.

Suppression of Mode Partition Noise by Laser Diode Light Injection

KATSUSHI IWASHITA AND KIYOSHI NAKAGAWA

Abstract—**This paper describes the improvement in mode partition noise characteristics when a laser light is injected into a laser diode modulated at 400 Mbits/s. A single-mode fiber transmission experiment is carried out for the 1.5 μm region. A 20 km repeater spacing at 400 Mbit/s modulation is achieved by LD light injection. The center longitudinal mode power is increased to 94 percent of the total modes. Relative noise in the center longitudinal mode is improved 30 dB by optical injection of −18.2 dBm. However, the mode partition noise generated by noninjected modes is not completely suppressed. The relationship between the half-power width of the spectral envelope and signal-to-noise ratio (SNR) degradation is obtained at 20 km fiber length. If 3 dB excess SNR degradation is allowed for the mode partition noise, then the necessary half-power width of the spectral envelope is less than 0.6 nm.**

Manuscript received February 17, 1982; revised June 9, 1982.
The authors are with the Yokosuka Electrical Communication Laboratory, Nippon Telegraph and Telephone Public Corporation, Yokosuka-shi, Kanagawa, Japan.

I. INTRODUCTION

SILICA-based optical fiber losses have been achieved at less than 1.0 dB/km from the 1.1-1.7 μm wavelength region [1]. There is a possibility of realizing several tens of kilometers of repeater spacing in a high bit rate using these low-loss single-mode fibers. However, when we use semiconductor laser diodes (LD's) as an optical source, the repeater spacing is restricted by the mode partition noise in a high bit rate [2]-[4]. For example, 20 km repeater spacing has not been achieved at 400 Mbits/s at 1.51 μm due to the influence of mode partition noise [5]. Although 44.3 km repeater spacing has been achieved at 2 Gbits/s at 1.3 μm in the dispersion free region, narrow spectral distribution is required [6]. Thus, the mode partition noise prevents the realization of high-speed transmission and wavelength division multiplexing transmission systems. Zero dispersion in low-loss wavelengths

0018-9480/82/1000-1657$00.75